Porous Teflon Ring–Solid Disk Electrode Arrangement for Differential Mass Spectrometry Measurements in the Presence of Convective Flow Generated by a Jet Impinging Electrode in the…

ARTICLE *in* ANALYTICAL CHEMISTRY · MAY 2012

Impact Factor: 5.64 · DOI: 10.1021/ac300799k · Source: PubMed

5 AUTHORS, INCLUDING:

Imre Treufeld
Case Western Reserve University
6 PUBLICATIONS **8** CITATIONS

SEE PROFILE

Denis Martins de Godoi
São Paulo State University
15 PUBLICATIONS **159** CITATIONS

SEE PROFILE

analytical chemistry

Letter

pubs.acs.org/ac

Porous Teflon Ring-Solid Disk Electrode Arrangement for Differential Mass Spectrometry Measurements in the Presence of Convective Flow Generated by a Jet Impinging Electrode in the Wall-Jet Configuration

Imre Treufeld, Adriel Jebin Jacob Jebaraj, Jing Xu, Denis Martins de Godoi, and Daniel Scherson*

The Ernest B. Yeager Center for Electrochemical Sciences and The Department of Chemistry, Case Western Reserve University, Cleveland, Ohio 44106-7078, United States

Supporting Information

ABSTRACT: A porous Teflon ring|solid disk electrode is herein described specifically designed for acquiring online mass spectrometric measurements under well-defined forced convection created by liquid emerging from a circular nozzle impinging on the disk under wall-jet conditions. Measurements were performed for the oxidation of hydrazine, N_2H_4, in a deaerated phosphate buffer electrolyte (pH 7) on Au, a process known to yield dinitrogen as the product. The N_2^+ ion currents, measured by the mass spectrometer, $i(N_2^+)$, as well as the corresponding polarization curves recorded simultaneously displayed very similar s-like shapes when plotted as a function of the potential applied to the Au disk. In fact, the limiting currents observed both electrochemically and spectrometrically were found to be proportional to $[N_2H_4]$. However, the limiting values of $i(N_2^+)$ did not increase monotonically with the flow rate, ν_f, reaching instead a maximum and then decreasing to values independent of ν_f. This behavior has been attributed in part to hindrances in the mass transport of gases through the porous materials.

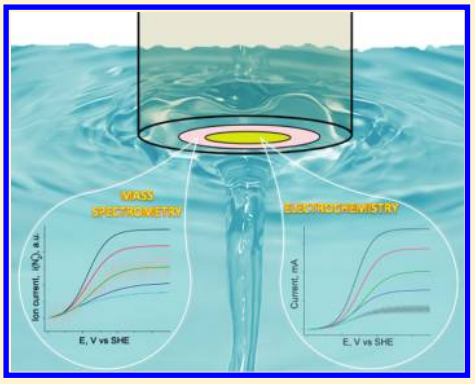

Since its inception about 4 decades ago,[1] the coupling of electrochemical systems with online mass spectrometry has provided valuable information regarding the mechanism of a growing number of reactions of fundamental and applied interest.[2,3] A variety of cell configurations have been devised allowing in most cases gases generated either directly or indirectly by electrochemical reactions to permeate through a porous membrane or plug, mostly made of Teflon, into an evacuated chamber that houses the mass spectrometer.[1,3−15] Of particular relevance to this work are strategies that combine the virtues of mass spectrometry with those of mass transport of the liquid electrolyte under forced convection.[5,7,9,11,12] Efforts in this direction have been reported by Tegtmeyer et al.,[9] who described a rotating porous metal disk electrode and established correlations between the Faradaic current and the ion current measured by the mass spectrometer, which were then used to calculate collection efficiencies. More recently, Heinen et al.[6] coupled online differential electrochemical mass spectrometry (DEMS) with in situ attenuated total reflection infrared spectroscopy in a channel-type dual thin-layer electrochemical flow-cell allowing simultaneous detection of gas phase products as well as stable solution phase and reactive adsorbed species. Directly relevant to our work is the report of Wang et al.,[11] who developed a double-band electrode channel cell, separated by a coplanar porous Teflon membrane. This arrangement made it possible to monitor not only gases but also electrochemically generated electroactive species.

The present contribution describes a novel assembly that enables gaseous species produced at a solid Au disk electrode under well-defined jet impinging conditions to permeate through a concentric porous Teflon ring membrane supported on a porous Teflon annulus, into the mass spectrometer chamber. The virtues of this device have been illustrated using the oxidation of hydrazine, N_2H_4, in an aqueous electrolyte, a process known to yield dinitrogen as the product.[15,16]

EXPERIMENTAL SECTION

The ring-disk probe specifically designed for online mass spectrometric measurements under well-defined forced convection generated by a jet impinging electrolyte consists of four main components (see panel A, Figure 1): a solid Au cylinder 0.5 cm in diameter (area, 0.196 cm^2) and 0.75 cm in height, a Teflon membrane (80 μm thick, thread seal tape from Fel-Pro Inc.), which was stretched to form a disk about 2 cm in diameter, a porous PTFE annulus (1−2 μm pore size, Porex) of outer diameter, 0.73 cm, inner diameter, 0.45 cm, and a solid PTFE holder in the form of a hollow cylinder (1.75 cm outer

Received: March 21, 2012
Accepted: May 26, 2012
Published: May 26, 2012

   dx.doi.org/10.1021/ac300799k | Anal. Chem. 2012, 84, 5175−5179

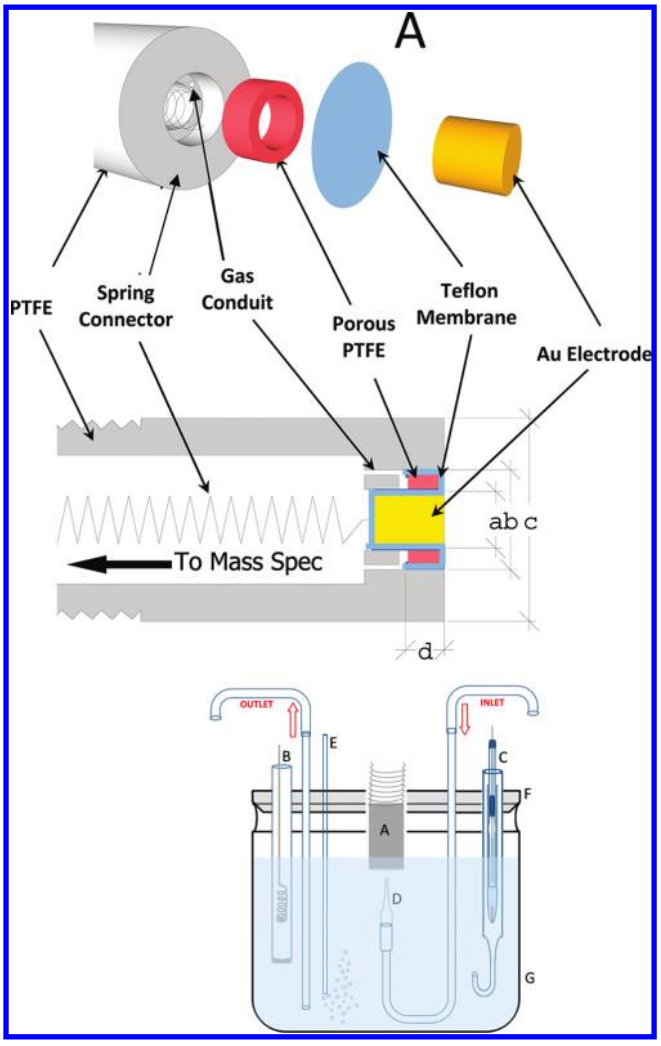

Figure 1. (Top panel) Components of the porous Teflon ringlAu disk electrode probe, A. (Middle panel) Cross section of the assembled probe, where a = 0.5 cm, b = 0.7 cm, c = 0.18 cm, d = 0.3 cm. (Lower panel) Schematic diagram of the electrochemical cell for online mass spectrometric measurements under forced convection generated by a jet impinging electrode: (A) porous Teflon ringlAu disk probe, (B) auxiliary electrode, (C) reference electrode, (D) jet nozzle, (E) bubbler, (F) Teflon lid, (G) glass cell.

diameter, 4.6 cm long). The porous annulus was cut out from a 0.32 cm thick porous PTFE sheet using a custom-built stainless steel tool comprised of two concentric stainless steel hollow rods with sharpened edges (o.d. 0.72 cm, i.d. 0.46 cm). All components were precision machined to form a water-tight seal.

Online mass spectrometric measurements were performed by immersing the ring-disk probe into ∼400 mL of electrolyte solution (*vide infra*) in an ∼500 mL cell (see lower panel, Figure 1) with the electrode facing down directly in front of the tip of a nozzle (i.d. 1.52 and o.d. 1.91 mm) aligned along an axis normal to the flat surface of the probe. Adjustments were made to position the nozzle pointing to the center of the Au disk about 4 mm from its surface. About 400 mL of electrolyte solution was forced to flow through a u-type tubing manifold ending in the immersed nozzle using a valveless piston pump (FMI) (see Figure 1). During operation, the column of liquid emerging from the nozzle impinged on the electrode and then spread radially along the surface of the probe bringing dissolved gaseous species in contact with the Teflon membrane. The actual volume of electrolyte in the cell at any given time was of about 300 mL. The flow rate was calibrated prior to the actual experiments by measuring the volume of the solution delivered per unit time. A Au foil (2.5 cm^2) and a standard hydrogen electrode (SHE) were used as auxiliary and reference electrodes, respectively.

The first step in the assembly of the ring-disk probe involves wrapping the Teflon membrane around the porous PTFE annulus followed by insertion of the Au electrode into the hollow section of the annulus. The latter is then pressed into a cavity in the solid PTFE holder (middle panel, Figure 1) making sure the front surface of the disk as well as that of the Teflon supported membrane and the PTFE annulus lie on a single common plane as required for achieving a well-defined hydrodynamic flow. It should be stressed that the use of a Teflon membrane was found to be essential, as no gases could be detected using only the porous plug under otherwise identical conditions. As shown in the figure, the back of the Au electrode is also pressed fit into a ledge made in the PTFE hollow cylinder. Gases present in the solution adjacent to the annulus surface permeate through the Teflon membrane and the porous Teflon annulus reaching a small void space adjacent to the wall of the Au cylinder and diffuse through two holes

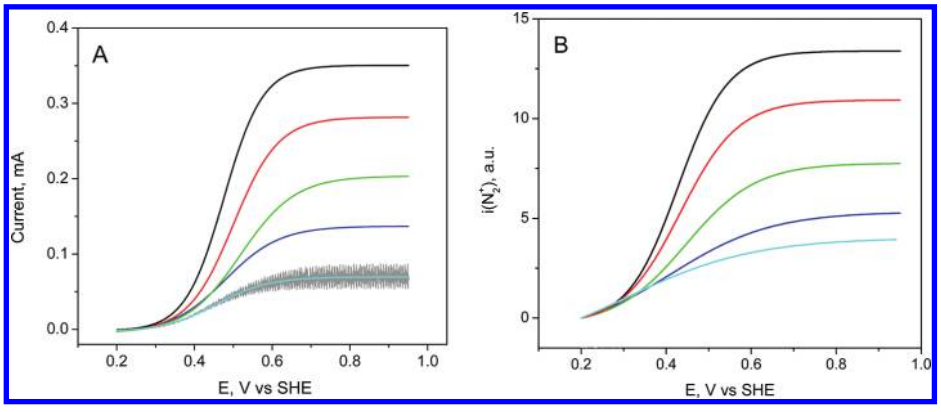

Figure 2. (A) Best-fit polarization curves collected with a Au disk (0.196 cm^2) at a rate of 5 mV/s, while flowing a 0.1 M PB (pH 7) containing hydrazine (N_2H_4) at different concentrations, i.e., 0.2 (cyan), 0.4 (blue), 0.6 (green), 0.8 (red), and 1.0 mM (black), at a rate ν_f = 0.081 cm^3/s. For clarity, only scans toward negative potentials are displayed. The jagged line represents the raw current for data collected in the 0.2 mM N_2H_4 solution in PB. (B) Best fit $i(N_2^+)$ vs E curve acquired simultaneously with curves in panel A.

dx.doi.org/10.1021/ac300799k | *Anal. Chem.* 2012, 84, 5175−5179

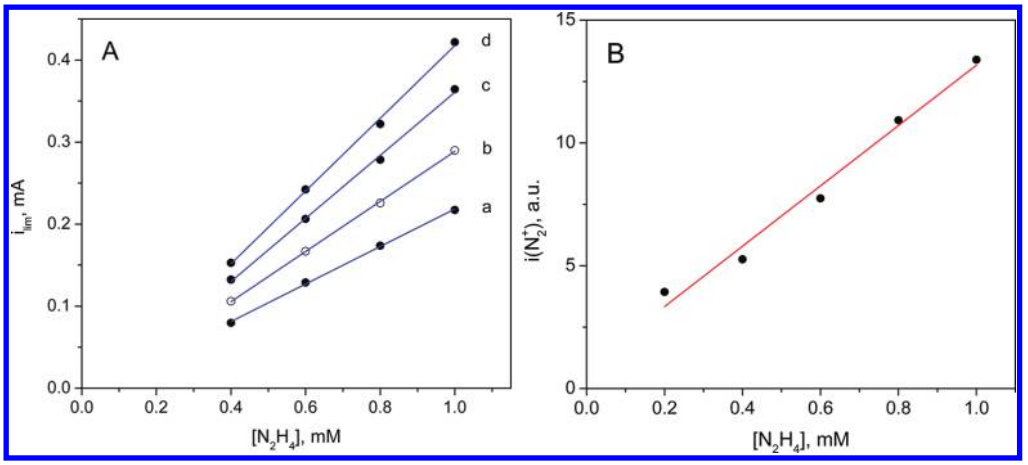

Figure 3. (A) Plots of Au disk limiting currents as a function of $[N_2H_4]$ for four different flow rates 0.048 (a), 0.081 (b), 0.112 (c), and 0.143 (d) cm^3/s. The best linear fits to the data are as follows: (a) slope $S = 2.29 \times 10^{-4}$, intercept, $I = -1.02 \times 10^{-5}$; (b) $S = 3.05 \times 10^{-4}$, $I = -1.64 \times 10^{-4}$; (c) $S = 3.84 \times 10^{-4}$, $I = -2.35 \times 10^{-4}$; (d) $S = 4.43 \times 10^{-4}$, $I = -2.55 \times 10^{-5}$. $R^2 > 0.997$ for all four sets of data. (B) Plot of the limiting ion current as a function of $[N_2H_4]$ recorded at $\nu_f = 0.081$ cm^3/s. $S = 12.46$ mM^{-1}; $I = 0.697$; $R^2 = 0.988$.

drilled on the ledge parallel to the main axis of the cylinder connected in turn to the mass spectrometer chamber. Contact to the working electrode was made by means of a spring as shown in the middle panel, Figure 1.

The mass-spectrometer employed for these studies was a Dycor Quadlink Q100 M (Ametek) with Dycor 2000 software. The small chamber that housed the mass spectrometer was evacuated using a Leybold Turbovac 50 turbomolecular pump backed by a Leybold Trivac roughing pump. During the measurements the pressure inside the vacuum system was of about 2×10^{-5} Torr. The N_2 signal ($m/z = 28$), $i(N_2^+)$, was collected with a dwell time of 15 ms and the data was acquired at a rate of ~11 points/s.

Experiments were performed in deaerated (Ar purged) hydrazine (monohydrate, Sigma-Aldrich, reagent grade, 100.4%) solutions in the range 0.2 to 1 mM in 0.1 M phosphate buffer (PB, pH 7) prepared from monosodium dihydrogen phosphate ($NaH_2PO_4 \cdot H_2O$, Ultrapure, J. T. Baker, 99.9%) and disodium phosphoric acid (Na_2HPO_4, Ultrapure, J. T. Baker, 99.7%) and ultrapure water (18.3 MΩcm, EASY-pureUV system, Barnstead) at room temperature. Potential control was achieved with a Pine potentiostat (RDE4) which was in turn connected via a data acquisition card (National Instruments, USB-6009) to a personal computer. Data were collected at a rate of 1000 points/s and stored as the adjacent average of 250 points/s referred to hereafter as the raw data.

RESULTS AND DISCUSSION

Shown in panel A, Figure 2 are the best-fit polarization curves obtained for the Au disk of the probe recorded at a rate of 5 mV/s, while flowing a 0.1 M PB (pH 7) containing hydrazine (N_2H_4) at different concentrations, i.e., 0.2 (cyan), 0.4 (blue), 0.6 (green), 0.8 (red), and 1.0 mM (black), at a rate $\nu_f = 0.081$ cm^3/s, through the nozzle toward the center of the Au disk. For clarity, only scans toward negative potentials are displayed. The scattered points represent the raw current for data collected in the 0.2 mM N_2H_4 solution in PB, where the large amplitude oscillations are induced by the modulation in the flow rate introduced by the valveless piston pump. The latter was clearly evidenced in the Fourier transform of the data, which was characterized by a prominent sharp peak at precisely the same frequency as that of the rotor in the pump, i.e., 0.38 Hz (see Figure S1, Supporting Information).

A plot of the limiting current, i_{lim}, as a function of $[N_2H_4]$ yielded a straight line with a very small negative intercept (see open symbols in panel A of Figure 3). Also shown in this panel are data collected at three other values of ν_f (see solid symbols). It may thus be surmised that within the experimental conditions selected, the oxidation of N_2H_4 is first order in the reactant and that i_{lim} is strictly diffusion controlled. This behavior is in agreement with that reported by Yan et al.,[17] who obtained linear i_{lim} vs $[N_2H_4]$ plots using a rotating (nongas) porous Au electrode supported on glassy carbon in 0.1 M phosphate buffer (pH 8.5) for $[N_2H_4]$ in the range 0.1−10 μM.

The expression for i_{lim} for a jet impinging electrolyte in the wall jet configuration is given by[18]

$$i_{lim} = (1.60k)nFC^{\circ}D^{2/3}\nu^{-5/12}\nu_f^{3/4}a^{-1/2}R^{3/4} \quad (1)$$

where k is a constant, n, the number of electrons transferred, F, Faraday's constant, C° and D, the bulk concentration and the diffusion coefficient of the electroactive species respectively, ν, the kinematic viscosity, ν_f, the flow rate, a, the nozzle diameter, and R, the radius of the disk electrode. The value of D for N_2H_4, assuming $\nu = 0.0101$ cm^2/s, was determined from data collected from polarization curves recorded with a Au rotating disk electrode as a function of rotation speed for $[N_2H_4] = 0.2$ mM (see Figure S2 in the Supporting Information), yielding a value of 1.33×10^{-5} cm^2/s, which is in excellent agreement with that published in the literature.[17,19] The general validity of eq 1 was assessed by calculating k based on the entire set of experimental data, yielding an average value of 0.868 ± 0.032. This value compares very well with that reported by Yamada and Matsuda, i.e., 0.86,[18] which provides strong evidence for the reliability of the hydrodynamic characteristics of the device.

Corresponding best fits to $i(N_2^+)$ vs the applied potential E acquired simultaneously (see panel B, Figure 2) displayed the same overall trend as the polarization curves, including clearly defined limiting values in the positive potential range. Also shown in this panel is the raw data for 0.6 mM N_2H_4 (see scattered points). It is thus of interest from an analytical viewpoint to establish whether $i(N_2^+)$ is proportional to the amount of N_2 generated at the disk using the data in Figure 2. To this end, the two signals were normalized to their

dx.doi.org/10.1021/ac300799k | Anal. Chem. 2012, 84, 5175−5179

corresponding limiting values. However, for this and all other concentrations examined, the plots of the best fits values for the normalized $i(N_2^+)$ do not overlap their normalized current counterparts, as illustrated in Figure 4 for $[N_2H_4]$ = 0.8 mM,

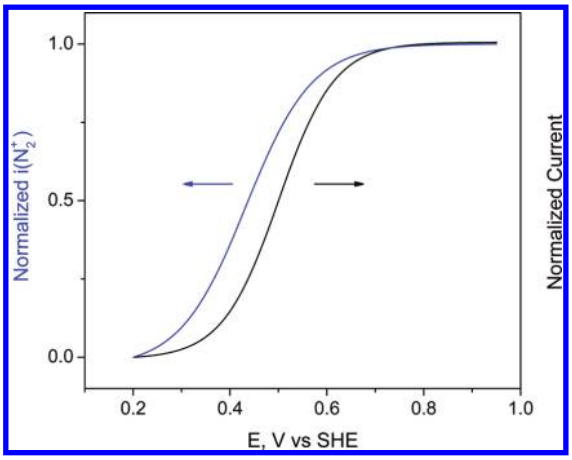

Figure 4. Normalized best fit dynamic polarization (blue) and $i(N_2^+)$ vs E curves based on data recorded simultaneously in a 0.8 mM N_2H_4 in PB (pH 7) solution at ν_f = 0.081 cm^3/s.

clearly indicating the two signals are not proportional in the full potential range. This may not be surprising as the porous Teflon ring does not behave as the solid ring of a conventional rotating ring disk electrode (RRDE), for which its potential is set to a value where the redox reaction proceeds under strict diffusion control. Specifically, the thickness of the diffusion boundary layer and thus the concentration profile of the dissolved gas along the surface of the porous annulus is nonuniform. Under these conditions, a theoretical analysis of the $i(N_2^+)$ curves, not as yet available, will be far more involved than for a conventional RRDE. Rather unexpectedly, however, a plot of $i(N_2^+)$ recorded at i_{lim} as a function of $[N_2H_4]$ (panel B, Figure 3) for ν_f = 0.081 cm^3/s, was nevertheless found to be fairly linear.

Two additional observations point to the complexities associated with this system: (i) The average $i(N_2^+)$ (see black symbols, left ordinate, Figure 5) increased with flow rate,

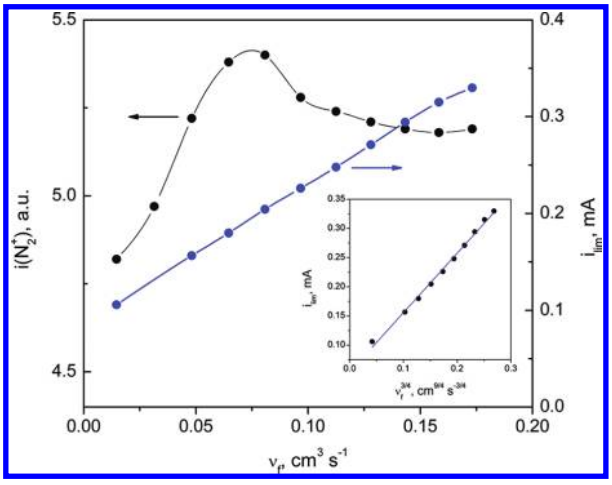

Figure 5. Plot of $i(N_2^+)$ as a function of the flow rate, ν_f, recorded in a solution 0.6 mM N_2H_4 in 0.1 M PB (pH 7). Insert. Plot of i_{lim} vs $\nu_f^{3/4}$ based on data collected simultaneously (see text for details).

attained a maximum at ν_f ~0.08 cm^3/s, and decreased slowly thereafter to reach a fairly constant value at higher ν_f. This phenomenon is unrelated to the electrochemical response, as a plot of i_{lim} vs $\nu_f^{3/4}$ (see insert in this figure), based on the values of i_{lim} as a function of ν_f recorded simultaneously (see blue symbols, right ordinate in Figure 5) was linear, as predicted by eq 1. (ii) Significant deviations from the linear behavior were reported by Wang et al. for measurements of the ion currents in aqueous solutions saturated with carbon dioxide and argon upon increasing the flow rate.[11] More specifically, the response of the mass spectrometer was smaller than that extrapolated from the lower flow rates as would be expected for mass transport hindrances through the membrane and/or porous plug.

CONCLUDING REMARKS

The porous Teflon ring|Au disk electrode assembly described in this letter made it possible to conduct online mass spectrometric measurements under well-defined forced convection conditions generated by a jet impinging electrolyte using the oxidation of N_2H_4 on Au in an aqueous buffered electrolyte (pH 7) as a model system. Both the current and the mass spectrometric response, $i(N_2^+)$, as a function of the applied potential were sigmoidal, reaching limiting values at sufficiently high overpotentials, which showed a linear dependence with $[N_2H_4]$. Plots of $i(N_2^+)$ as a function of the flow rate, however, displayed a peak followed by a flat plateau at higher ν_f. This phenomenon was attributed to mass transport hindrances through the Teflon membrane and/or porous Teflon plug. A theoretical analysis of this system is currently being pursued and will be reported in due course.

ASSOCIATED CONTENT

Supporting Information

Additional information as noted in text. This material is available free of charge via the Internet at http://pubs.acs.org.

AUTHOR INFORMATION

Corresponding Author

*E-mail: dxs16@po.cwru.edu.

Notes

The authors declare no competing financial interest.

ACKNOWLEDGMENTS

Funds for this work were provided by a grant from NSF (Grant CHE-0911621).

REFERENCES

(1) Bruckenstein, S.; Gadde, R. *J. Am. Chem. Soc.* **1971**, *93*, 793.
(2) Baltruschat, H. *J. Am. Soc. Mass Spectrom.* **2004**, *15*, 1693−1706.
(3) Gun, J.; Bharathi, S.; Gutkin, V.; Rizkov, D.; Voloshenko, A.; Shelkov, R.; Sladkevich, S.; Kyi, N.; Rona, M.; Wolanov, Y.; Rizkov, D.; Koch, M.; Mizrahi, S.; Pridkhochenko, P. V.; Modestov, A.; Lev, O. *Isr. J. Chem.* **2010**, *50*, 360−373.
(4) Bogdanoff, P.; Friebe, P.; Alonso-Vante, N. *J. Electrochem. Soc.* **1998**, *145*, 576−582.
(5) Fujihira, M.; Noguchi, T. *J. Electroanal. Chem.* **1993**, *347*, 457−63.
(6) Heinen, M.; Chen, Y. X.; Jusys, Z.; Behm, R. J. *Electrochim. Acta* **2007**, *52*, 5634−5643.
(7) Planes, G. A.; Garcia, G.; Pastor, E. *Electrochem. Commun.* **2007**, *9*, 839−844.

(8) Smith, S. P. E.; Casado-Rivera, E.; Abruna, H. D. *J. Solid State Electrochem.* **2003**, *7*, 582−587.
(9) Tegtmeyer, D.; Heindrichs, A.; Heitbaum, J. *Ber. Bunsenges. Phys. Chem.* **1989**, *93*, 201−206.
(10) Volk, K. J.; Yost, R. A.; Brajter-Toth, A. *Anal. Chem.* **1992**, *64*, 21A−26A, 28A, 30A−33A.
(11) Wang, H.; Rus, E.; Abruna, H. D. *Anal. Chem.* **2010**, *82*, 4319−4324.
(12) Wasmus, S.; Cattaneo, E.; Vielstich, W. *Electrochim. Acta* **1990**, *35*, 771−5.
(13) Wonders, A. H.; Housmans, T. H. M.; Rosca, V.; Koper, M. T. M. *J. Appl. Electrochem.* **2006**, *36*, 1215−1221.
(14) Wuersig, A.; Scheifele, W.; Novak, P. *J. Electrochem. Soc.* **2007**, *154*, A449−A454.
(15) Rosca, V.; Koper, M. T. M. *Electrochim. Acta* **2008**, *53*, 5199−5205.
(16) Alvarez-Ruiz, B.; Gomez, R.; Orts, J. M.; Feliu, J. M. *J. Electrochem. Soc.* **2002**, *149*, D35−D45.
(17) Yan, X. L.; Meng, F. H.; Cui, S. Z.; Liu, J. G.; Gu, J.; Zou, Z. G. *J. Electroanal. Chem.* **2011**, *661*, 44−48.
(18) Yamada, J.; Matsuda, H. *J. Electroanal. Chem.* **1973**, *44*, 189−198.
(19) Karp, S.; Meites, L. *J. Am. Chem. Soc.* **1962**, *84*, 906−912.

dx.doi.org/10.1021/ac300799k | *Anal. Chem.* 2012, 84, 5175−5179